


## Article

# Theoretical Analysis of Vuilleumier's Hypothetical Engine and Cooler

Qi Liu <sup>1,2,3</sup>, Baojun Luo <sup>1,2,3,\*</sup>, Jiayao Yang <sup>1,2</sup> , Qun Gao <sup>1,2</sup>, Jingping Liu <sup>1,2,3</sup>, Yuexin Huang <sup>4</sup> and Chengqin Ren <sup>1,2</sup>

<sup>1</sup> State Key Laboratory of Advanced Design and Manufacturing for Vehicle Body, Hunan University, Changsha 410082, China; hnuliuiqi@hnu.edu.cn (Q.L.); yangjiy97@126.com (J.Y.); gaoq888@yeah.net (Q.G.); wavyt@msn.com (J.L.); renchengqin@163.com (C.R.)

<sup>2</sup> College of Mechanical and Vehicle Engineering, Hunan University, Changsha 410082, China

<sup>3</sup> Research Institute of Hunan University in Chongqing, Chongqing 401120, China

<sup>4</sup> Thermolift Inc., 209 Advanced Energy Center, 1000 Innovation Road, Stony Brook, NY 11794, USA; yuexin@thermoliftenergy.com

\* Correspondence: luobaojun@hnu.edu.cn; Tel.: +86-136-3749-2492

**Abstract:** Vuilleumier machines are a promising technology for heating. Respective performances of Vuilleumier's engine and cooler are generally unclear. In Stirling machines, performances can be determined based on PV power flow and heat flow methods. In this work, respective performances based on two methods in current Vuilleumier models were investigated. It was found that PV power flow and heat flow methods in current Vuilleumier models were ineffective for analysis of respective performances due to there being no piston as a boundary between Vuilleumier's engine and cooler. Then, a virtual piston was assumed, and a virtual piston based Vuilleumier model (VPBVM) was developed. The relative Carnot efficiencies of the obtained engine and cooler were 53~64% and 43~49%, respectively, at conditions of 550 °C hot temperature, 50~70 °C warm temperature, and −20~10 °C cold temperature. The results indicated that respective performances obtained in VPBVM were reasonable. Moreover, the engine's compression ratios could be obtained in VPBVM and were 1.2~1.24. Thus, VPBVM could be effective for the analysis of the Vuilleumier machine's engine and cooler.

**Keywords:** Vuilleumier cycle; Stirling engine; Stirling cooler; virtual piston; compression ratio



**Citation:** Liu, Q.; Luo, B.; Yang, J.; Gao, Q.; Liu, J.; Huang, Y.; Ren, C. Theoretical Analysis of Vuilleumier's Hypothetical Engine and Cooler. *Energies* **2021**, *14*, 5923. <https://doi.org/10.3390/en14185923>

Academic Editors: Bruno Facchini and Constantine D. Rakopoulos

Received: 21 July 2021

Accepted: 12 September 2021

Published: 18 September 2021

**Publisher's Note:** MDPI stays neutral with regard to jurisdictional claims in published maps and institutional affiliations.



**Copyright:** © 2021 by the authors. Licensee MDPI, Basel, Switzerland. This article is an open access article distributed under the terms and conditions of the Creative Commons Attribution (CC BY) license (<https://creativecommons.org/licenses/by/4.0/>).

## 1. Introduction

Vuilleumier machines are a promising technology for heating [1,2]. Figure 1 shows a schematic diagram of free piston Vuilleumier machines, which consist of displacers (hot  $D_h$  and cold  $D_c$ ), regenerators (hot ⑤ and cold ⑧), chambers (hot ①, warm ② and cold ③), and heat exchangers (hot ④, hot-warm ⑥, cold-warm ⑦, and cold ⑨). Although there is no piston, Vuilleumier machines are essentially a Stirling engine-driven Stirling cooler [3,4]. The coupling between the hypothetical Stirling engine and Stirling cooler is a working fluid.

As a Stirling cooler driven by a Stirling engine, its theoretical efficiency can achieve Carnot efficiency. However, in a practical Vuilleumier machine, the achieved coefficient of performance (COP) is much lower. Adiabatic losses, heat losses, and friction losses are the main reason for a low practical COP. Nevertheless, as thermal-to-mechanical efficiency in the independent Stirling engine and mechanical-to-thermal efficiency in the independent Stirling cooler can reach 68% [5] and 41~46% [6] of Carnot efficiency, respectively, Vuilleumier machines could have 28~31% of Carnot efficiency for cooling, which is the product of the independent Stirling engine and independent Stirling cooler values [7]. However, as shown in Table 1, the maximum relative Carnot efficiency  $COP_{Carnot}$  in practical Vuilleumier machines is only 15%, which is nearly half of the value based on an independent Stirling engine and independent Stirling cooler.

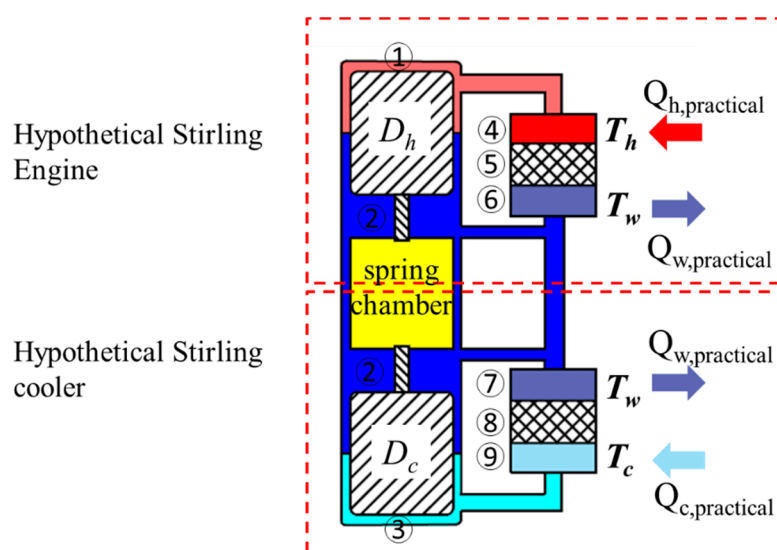


**Figure 1.** Schematic of free piston Vuilleumier machine.

**Table 1.** A summary of performance of Vuilleumier heat pumps.

Author	T <sub>c</sub> [K]	T <sub>w</sub> [K]	T <sub>h</sub> [K]	COP <sub>v</sub>	COP <sub>Cartnot</sub>
Kuhl [8]	263	313	773	0.161	0.05
Carlsen [1]	285	313	873	0.665	0.1
Kawajiri [9]	285	318	973	<0.7	<0.12
Pfeffer [10]	273	323	773	0.392	0.12
Kuhl [11]	262	306	853	0.571	0.15

At present, the engine's thermal efficiency and cooler's COP<sub>C</sub> in Vuilleumier machines are usually unknown. Thus, it is usually unclear whether a Vuilleumier's low overall performance is due to the engine's low thermal efficiency or cooler's COP<sub>C</sub> in Vuilleumier machines. Moreover, few studies have been carried out for the analysis of the Vuilleumier's engine and cooler, except our previous work [12]. In our previous work, an alternate method of combining an adiabatic sub-model with losses and an isothermal sub-model without losses is proposed. The results indicate that there is still room to improve the accuracy of the obtained respective performances. Thus, it is essential to carry out a further study analyzing the respective performances of a hypothetical Stirling engine and Stirling cooler, which could be helpful for revealing the characteristics of the Vuilleumier machine and provide a guide for the preliminary design and optimization of the Vuilleumier machine.

Basically, determinations of Stirling machines' performances can be experimentally and theoretically obtained based on two methods. One method is to monitor PV power flow in the chambers:

$$W = \oint PdV \quad (1)$$

The other method is to monitor heat flow in heat exchangers:

$$\frac{dQ}{d\varphi} = \frac{V \cdot \frac{\partial P}{\partial \varphi} \cdot C_v}{R} - C_p \cdot (T_{in} \cdot m_{in} - T_{out} \cdot m_{out}) \quad (2)$$

These methods have been popularly employed for the overall performance of Vuilleumier machines [13] and performance analysis of Stirling machines, such as the Stirling engine [14–16], Stirling cooler [17,18], and duplex Stirling machines [19]. It seems that PV

power flow and heat flow will be also effective in the performance analysis of Vuilleumier's hypothetical Stirling engine and Stirling cooler.

However, as the Stirling engine and Stirling cooler in a Vuilleumier machine are coupled by a working fluid, there is no piston to isolate the volumes of the engine and cooler. On the one hand, variations of these volumes in Equation (1) based on PV power flow are difficult to determine, due to there being no piston as a boundary between the engine's and cooler's volumes. On the other hand, the mixing of an engine's and cooler's working fluids in Vuilleumier's warm chamber will lead to a shift of heat flow in the engine's and cooler's warm heat exchangers, resulting from the heat transfer between the engine's and cooler's working fluids due to mixing. Thus, the effectiveness of PV power flow and heat flow methods in the performance analysis of Vuilleumier's hypothetical Stirling engine and cooler should be evaluated.

As stated above, the challenge of obtaining the respective performances in Vuilleumier machines is due to there being no piston, which leads to there being no boundary between the engine's and cooler's volumes. Thus, an assumed virtual piston could be a solution since it will provide a virtual boundary between the engine's and cooler's volumes. Then, respective performances can be obtained based on the PV power flow method or Equation (1). However, the method for tracking the virtual piston's position during the cycle needs to be studied.

In this work, both PV power flow and heat flow methods were first employed for the analysis of hypothetical Stirling engine's and Stirling cooler's performance in current Vuilleumier models. Then, a virtual piston was assumed in Vuilleumier machine. A method of tracking the position of a virtual piston in a current Vuilleumier model was proposed. Respective performances of the hypothetical Stirling engine and cooler were obtained and analyzed based on the developed virtual piston model.

## 2. Principles of Hofbauer's Vuilleumier Cycle Heat Pump

In conventional Vuilleumier machines, the motions of hot and cold displacer are always moving simultaneously. This will lead to lower specific output. Furthermore, its COP at partial load will be reduced as a result of the control strategy of on-off or reducing the hot temperature. In order to overcome these drawbacks, Hofbauer invented a four-process cycle Vuilleumier heat pump with electromechanically-actuated displacers [12,13,20,21]. The basic structure of Hofbauer's Vuilleumier cycle heat pump (HVCHP, as shown in Figure 2) is the same as that of conventional Vuilleumier cycle heat pump (as shown in Figure 1), except for the additional electromechanical component, which is not shown in Figure 2. As a result, the displacers can be controlled by the electromechanical components to be stationary at its bottom dead center (BDC) and top dead center (TDC) (as shown in Figure 2). Figure 2 shows the motions of displacers during a cycle. It can be found that the motions in HVCHP are noncontinuous and rise-dwell-fall-dwell. Thus, HVCHP can easily meet the partial load by reducing the operating cycles per second. Moreover, it could have a longer life as a result of fewer operating cycles at partial load and higher output at full load [12,13].

### 2.1. Current Adiabatic Vuilleumier Models

At present, there have been adiabatic and isothermal models for the analysis of Vuilleumier machines [22]. The difference between the two models is compression and expansion processes in the chambers. These processes are assumed to be adiabatic in the adiabatic model while isothermal in the isothermal model. Generally, the adiabatic model has much higher accuracy. Thus, the current adiabatic Vuilleumier model is employed as the baseline. Moreover, the following assumptions are made: no pressure drop in the working space; ideal gas; constant temperature in the hot, warm, and cold heat exchangers, and constant average temperature in the regenerators. The working fluid in warm chamber has the same temperature.

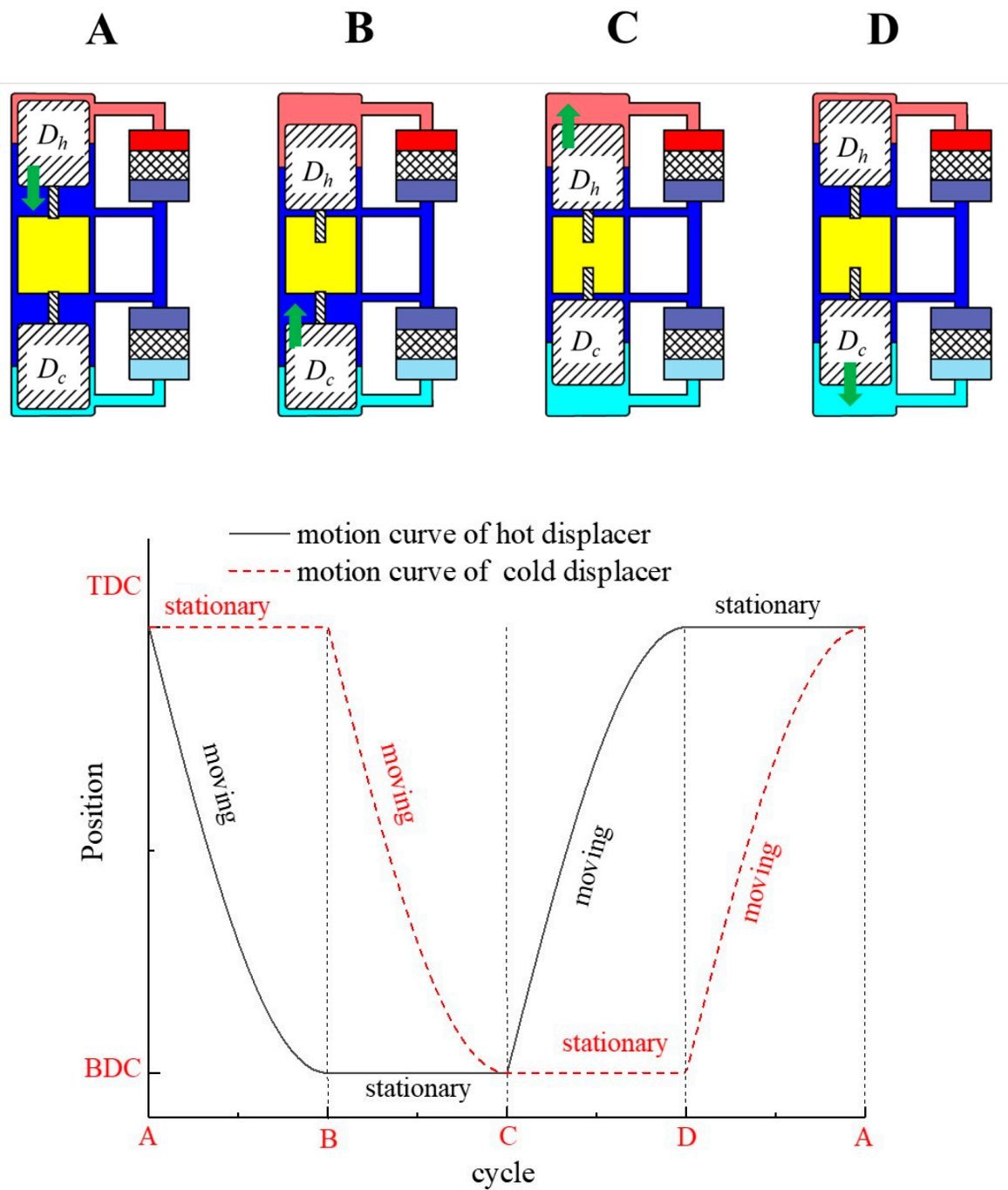


**Figure 2.** Schematic of motions of displacers in HVCHP.

#### 2.1.1. Variations of Working Fluid's Mass in Respective Components

For the heat exchangers and regenerators with constant volumes, the variations of the working fluid's mass are determined by

$$dm_i = \frac{V_i}{RT_i} dP \quad (i = 4, 5, 6, 7, 8, 9) \quad (3)$$

For the hot, warm, and cold chambers with variable volumes, the variations of the working fluid's mass are determined by

$$dm_i = \frac{PdV_i + \frac{1}{\gamma} V_i dP}{RT_i^*} \quad (i = 1, 2, 3) \quad (4)$$

where  $\gamma$  is the ratio of specific heat and  $T_i^*$  are temperature that the working fluid flowing into or out the chamber, which is shown in Figure 3 and are determined by

$$T_{he} = \begin{cases} T_h & (dm_{he} > 0) \\ T_1 & (dm_{he} < 0) \end{cases} \quad (5)$$

$$T_{wc} = \begin{cases} T_w & (dm_{ce} < 0) \\ T_2 & (dm_{ce} > 0) \end{cases} \quad (6)$$

$$T_{ce} = \begin{cases} T_c & (dm_{ce} > 0) \\ T_3 & (dm_{ce} < 0) \end{cases} \quad (7)$$

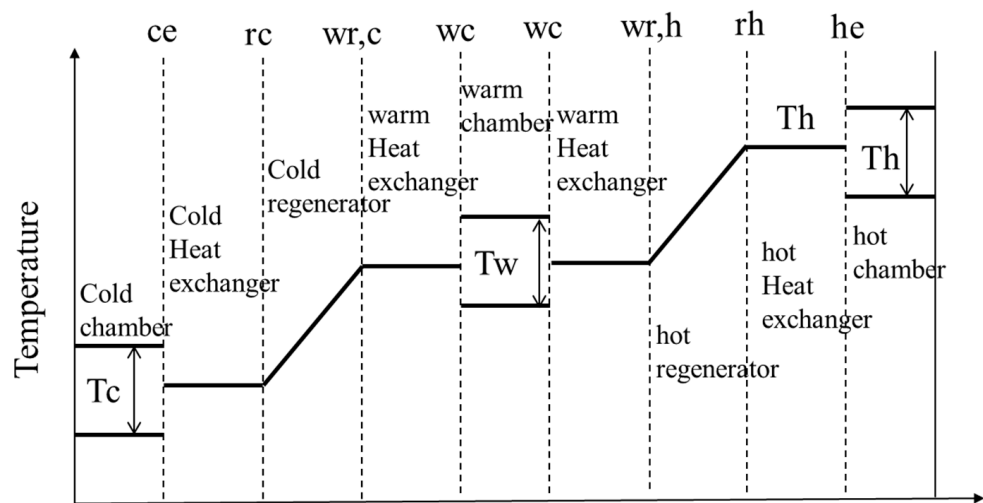


Figure 3. Temperatures in Vuilleumier machines.

#### 2.1.2. Variations of Pressure

The pressure is determined based on  $\sum_{i=1}^9 dm_i = 0$ . Thus, based on Equations (3) and (4), the pressure can be obtained by

$$dP = - \frac{\frac{PdV_1}{T_1^*} + \frac{PdV_2}{T_2^*} + \frac{PdV_3}{T_3^*}}{\frac{V_4}{T_4^*} + \frac{V_5}{T_5^*} + \frac{V_6}{T_6^*} + \frac{V_7}{T_7^*} + \frac{V_8}{T_8^*} + \frac{V_9}{T_9^*} + \frac{V_1}{\gamma T_1^*} + \frac{V_2}{\gamma T_2^*} + \frac{V_3}{\gamma T_3^*}} \quad (8)$$

#### 2.1.3. Variations of Temperatures in Hot, Warm and Cold Chambers

The variations of temperatures can be determined according to the ideal gas law  $PV = mRT$ .

$$\frac{dT_i}{T_i} = \frac{dV_i}{V_i} + \frac{dP}{P} - \frac{dm_i}{m_i} \quad (i = 1, 2, 3) \quad (9)$$

#### 2.1.4. PV Power Flow in Hot, Warm and Cold Chambers

The indicated PV power flow can be determined based on PV power flow:

$$W_h = \int PA_h dx_h \quad (10)$$

$$W_c = \int PA_c dx_c \quad (11)$$

$$W_{w,h} = \int PA_{w,h} dx_h \quad (12)$$

$$W_{w,c} = \int PA_{w,c} dx_c \quad (13)$$

Furthermore, in order to approach a practical performance, regenerator loss  $Q_R$ , shuttle loss  $Q_{shuttle}$ , and conduction loss  $Q_{con}$  are considered. The detailed calculations can be found in the literature [12,19]. Thus, the practical absorbed heat in the cold and hot heat exchangers can be determined by

$$Q_{c,practical} = W_c - Q_{R,C} - Q_{shuttle,C} - Q_{con,C} \quad (14)$$

$$Q_{h,practical} = W_h + Q_{R,E} + Q_{shuttle,E} + Q_{con,E} \quad (15)$$

### 2.1.5. Heat Flow in Hot, Warm and Cold Heat Exchangers

The indicated absorbed heat in the heat exchangers can be determined based on heat flow:

$$\frac{dQ_h}{d\varphi} = \frac{V_h \cdot \frac{\partial P}{\partial \varphi} \cdot C_v}{R} - C_p \cdot (T_{rh} \cdot m_{rh} - T_{he} \cdot m_{he}) \quad (16)$$

$$\frac{dQ_{w,h}}{d\varphi} = \frac{V_{w,h} \cdot \frac{\partial P}{\partial \varphi} \cdot C_v}{R} - C_p \cdot (T_{wc,h} \cdot m_{wc,h} - T_{wr} \cdot m_{wr,h}) \quad (17)$$

$$\frac{dQ_{w,c}}{d\varphi} = \frac{V_{w,c} \cdot \frac{\partial P}{\partial \varphi} \cdot C_v}{R} - C_p \cdot (T_{wc,c} \cdot m_{wc,c} - T_{wr} \cdot m_{wr,c}) \quad (18)$$

$$\frac{dQ_c}{d\varphi} = \frac{V_c \cdot \frac{\partial P}{\partial \varphi} \cdot C_v}{R} - C_p \cdot (T_{rc} \cdot m_{rc} - T_{ce} \cdot m_{ce}) \quad (19)$$

Moreover, the practical absorbed heat in the cold and hot heat exchangers can be determined by

$$Q_{c,practical} = Q_c - Q_{R,C} - Q_{shuttle,C} - Q_{con,C} \quad (20)$$

$$Q_{h,practical} = Q_h + Q_{R,E} + Q_{shuttle,E} + Q_{con,E} \quad (21)$$

### 2.1.6. Overall Performance of Vuilleumier

Vuilleumier's overall performance can be determined by

$$COP_V = Q_{c,practical} / Q_{h,practical} \quad (22)$$

where subscript "V" represents the Vuilleumier machine.

### 2.1.7. Performance of Vuilleumier's Engine and Cooler

Current Vuilleumier model or Equations (3)–(22) has been validated to be effective for Vuilleumier's overall performance [23,24]. At present, few studies have been carried out for the analysis of the hypothetical Stirling engine and cooler. Thus, there are no formulas for the analysis of the hypothetical Stirling engine and cooler in the current Vuilleumier model. In this work, the respective performances based on the current Vuilleumier model are analyzed based on

$$W_E = Q_h - Q_{w,h} - W_{r,h} \text{ or } W_h - W_w - W_{r,h} \quad (23)$$

$$W_C = Q_{w,c} - Q_c + W_{r,c} \text{ or } W_w - W_c + W_{r,c} \quad (24)$$

$$\eta_E = \frac{Q_h - Q_{w,h} - W_{r,h}}{Q_h + Q_{loss,h}} \text{ or } \frac{W_h - W_w - W_{r,h}}{W_h + Q_{loss,h}} \quad (25)$$

$$COP_C = \frac{Q_c - Q_{loss,c}}{Q_{w,c} - Q_c + W_{r,c}} \text{ or } \frac{W_c - Q_{loss,c}}{W_w - W_c + W_{r,c}} \quad (26)$$

An engine's work output or cooler's work input is calculated based on indicated PV power flow or indicated heat flow. Related heat losses are considered in calculations of absorbed heat in the engine's hot heat exchanger and cooler's cold heat exchanger.

It should be pointed out that Equations (23)–(26) could be ineffective since it is assumed that all the heat in a hot-warm heat exchanger is all an engine's waste heat or the virtual boundary between the engine and cooler is always at the middle of the warm chamber.

#### 2.1.8. Four Chambers Model with Two Separate Warm Chambers

The above model is based on a Vuilleumier machine with three chambers, six heat exchangers, and three variable volume spaces. However, this Vuilleumier machine was also divided into ten functional spaces in some studies [22], with six heat exchangers and four variable volume spaces. The warm temperature chamber is considered to consist of two separate warm chambers (as shown in Figure 4). Furthermore, the working fluids' temperatures in two warm chambers are independent.

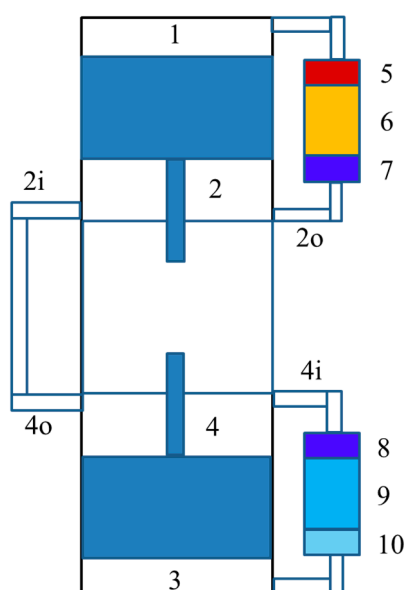


Figure 4. Schematic of four chambers Vuilleumier model.

The respective performances in the Vuilleumier model with four chambers is completely the same as the Vuilleumier model with three chambers, except for the determination of the pressure, which is calculated by

$$dP = \frac{\frac{PdV_4}{R_g} - T_4 \frac{PdV_3}{R_g T_3^*} + T_{4i} \left( \frac{PdV_1}{R_g T_1^*} + \frac{PdV_2}{R_g T_2^*} \right)}{T_4 \left( \frac{V_8}{R_g T_8} + \frac{V_9}{R_g T_9} + \frac{V_{10}}{R_g T_{10}} + \frac{1}{R_g} \frac{V_3}{T_3^*} \right) - \frac{1}{R_g} \frac{V_4}{T_4} - T_{4i} \left( \frac{V_5}{R_g T_5} + \frac{V_6}{R_g T_6} + \frac{V_7}{R_g T_7} + \frac{1}{R_g} \frac{V_1}{T_1^*} + \frac{1}{R_g} \frac{V_2}{T_2^*} \right)} \quad (27)$$

## 2.2. Improved Vuilleumier Model: Virtual Piston Based Vuilleumier Model

### 2.2.1. Assumption of Virtual Piston

As there is no real piston in Vuilleumier machines as a boundary between the engine and cooler, a virtual piston with zero volume and zero mass between the engine and cooler is assumed. The pressures in the engine's and cooler's warm chambers are the same as a result of there being no mass while the heat transfer between the working fluids across the virtual piston will not be isolated. Thus, the engine's PV work is transferred to the cooler by the virtual piston. On the one hand, as the virtual piston has zero volume, the position of the virtual piston (as shown in Figure 5) could be in the hot-warm heat exchanger, hot-warm chamber (as shown in Figure 5a), cold-warm chamber (as shown in Figure 5a), cold-warm heat exchanger, or cold regenerators (as shown in Figure 5c), depending on the operating conditions and the angle during the cycle. On the other hand, as the virtual piston will move through different cross-sections of the machine, the "shape"

of the virtual piston is assumed to be dependent on where it is in the machine. Overall, the above assumptions are reasonable.

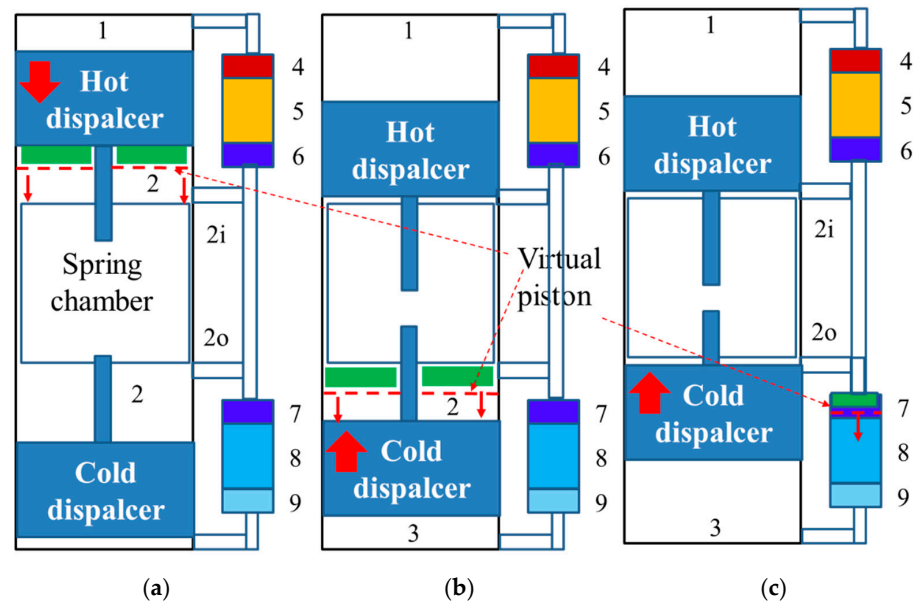


**Figure 5.** Schematic of Vuilleumier model with virtual piston.

### 2.2.2. Model for Engine's Output Work

If the position of the virtual piston during a cycle is determined, the engine's volume is also determined. Then, the engine's output work can be obtained by

$$dW_E = PdV_E \quad (28)$$

According to the ideal gas law for an engine's working fluids

$$PV = mRT \quad (29)$$

Its differential form is

$$PdV_E + V_E dP = Rd(mT) \quad (30)$$

Thus, Equation (28) becomes

$$dW_E = Rd(mT)_E - V_E dP \quad (31)$$

As there are multi masses and temperatures in engine, Equation (31) becomes

$$dW_E = R \sum_i (m_i dT_i + T_i dm_i)_E - V_E dP \quad (32)$$

where subscript "i" represents the engine's components marked in Figure 5. Thus, the position of the virtual piston should be determined first.

### 2.2.3. Method of Tracking the Position of Virtual Piston

In this work, a method of tracking the position of the virtual piston based on the engine's total working fluid mass is proposed. As the pressure is maximum at the end of A-B process or at 90° (as shown in Figure 2), the working fluid in the hot chamber ①, hot heat exchanger ④, hot regenerator ⑤ and hot-warm heat exchanger ⑥ is considered the engine's total working fluid at 90°. The engine's total working fluid mass is obtained in the current Vuilleumier model.

$$m_E = (m_1 + m_4 + m_5 + m_6)_{90^\circ} \quad (33)$$

where subscripts “1”, “4”, “5”, and “6” represent the components marked in Figure 5. Then, the position of the virtual piston during the cycle is tracked by determining the volume occupied by  $m_E$ .

#### Tracking the Position of Virtual Piston during the Process of 0~90°

During the process of 0~90° (as shown in Figure 2), the virtual piston is tracked and positioned in the warm chamber ② (as shown in Figure 5a). It should be pointed out that the mass of working fluids in the warm chamber ② consists of the engine's and cooler's working fluids. Thus, the part of the engine's working fluid  $m_{2E}$  stored in the warm chamber during the process can be determined based on the obtained total mass of the engine's working fluids according to Equation (33).

$$m_{2E} = m_E - (m_1 + m_4 + m_5 + m_6)_\varphi \quad (34)$$

where  $m_E$  is the engine's total working fluid and determined according to Equation (33),  $\varphi$  is the angle at the position, and subscript “2E” represents volume occupied by engine in warm chamber, which is marked in green in Figure 5a.

Then, the volume occupied by the engine's working fluid in the warm chamber can be obtained based on the ratio of an engine's mass of working fluid over the total mass of working fluid in the warm chamber.

$$V_{2E} = \frac{m_{2E}}{m_2} \cdot V_2 \quad (35)$$

Incorporating Equations (34) and (35), Equation (32) becomes

$$dW_E = R(m_1dT_1 + T_1dm_1 + \sum_{i=4-6} T_idm_i + m_{2E}dT_2 + T_2dm_{2E}) - (V'_E + V_{2E})dP \quad (36)$$

where  $V'_E$  is

$$V'_E = V_1 + V_4 + V_5 + V_6 \quad (37)$$

Thus, the engine's work output during the process of 0~90° can be determined according to Equation (36).

#### Tracking the Position of Virtual Piston during the Process of 90~180°

During the process of 90~180°, the virtual piston could move into the cold-warm heat exchanger ⑦ (as shown in Figure 5c) or cold regenerator ⑧. Thus, the ultimate position of virtual piston should be judged by

$$m_{2E} = \begin{cases} m_E - (m_1 + m_4 + m_5 + m_6 + m_2)_\varphi > 0 & (a) \\ m_E - (m_1 + m_4 + m_5 + m_6 + m_2 + m_7)_\varphi > 0 & (b) \end{cases} \quad (38)$$

If it is Equation (38a), the ultimate position is in the cold-warm heat exchanger ⑦. Thus, the volume occupied by the engine's working fluid in the cold-warm heat exchanger can be obtained by

$$V_{7E} = \frac{m_{7E}}{m_7} \cdot V_7 \quad (39)$$

$$m_{7E} = m_E - (m_1 + m_4 + m_5 + m_6 + m_2)_\varphi \quad (40)$$

where subscript “7E” represents the volume occupied by the engine in the cold-warm heat exchanger, which is marked in green in Figure 5c. Then, the engine's work output becomes

$$dW_E = R(\sum_{i=1,2,4-6} (m_idT_i + T_idm_i) + T_7dm_{7E}) - (V'_E + V_2 + V_{7E})dP \quad (41)$$

If it is Equation (38b), the ultimate position is in the cold regenerator ⑧. The volume occupied by the engine's working fluid in the cold regenerator is relatively difficult because

the temperature in the regenerator varies with the length. Firstly, the engine's mass in the regenerator is obtained.

$$m_{8E} = m_E - (m_1 + m_4 + m_5 + m_6 + m_2 + m_7)_\varphi \quad (42)$$

where subscript "8E" represents volume occupied by engine in cold regenerator. As the temperature in regenerator varies with the length, the regenerator is divided into N components. Then, the position in the regenerator is obtained by integral.

$$m_{8E} = \sum \frac{PV_j}{RT_j} \quad (43)$$

where subscript "j" represents j components. Thus, the engine's work output becomes

$$dW_E = R \left( \sum_{i=1,2,4-7} (m_i dT_i + T_i dm_i) + T_{8E} dm_{8E} + m_{8E} dT_{8E} \right) - (V'_E + V_2 + V_7 + V_{8E}) dP \quad (44)$$

#### Tracking the Position of Virtual Piston during the Process of 180~360°

During the process of 180~270°, the motion of virtual piston is the reverse process of 90~180°. During the process of 270~360°, the motion of the virtual piston is the reverse process of 0~90°. Similarly, the work output can be determined based on Equations (36), (41) and (44).

#### 2.2.4. Difference between Virtual Piston Based Vuilleumier Model and Current Vuilleumier Model

The pressure and temperatures in the chambers are determined by Equations (9) and (27), which are the same as those in current Vuilleumier model. Thus, the adsorbed heat in the engine's hot heat exchanger and cooler's cold heat exchanger will be the same. The difference between the virtual piston based Vuilleumier model and current Vuilleumier models is the determination of work (as shown in Table 2). As the variations of an engine's total volume can be determined due to the virtual piston, the work is determined based on Equation (28) in the virtual piston based Vuilleumier model. However, the work in the current Vuilleumier models cannot be determined by Equation (28) since the variations of the engine's total volume cannot be determined in current Vuilleumier models. Thus, it is determined based on Equations (23) and (24). A flowchart of the simulation process for the virtual piston based Vuilleumier model is shown in Figure 6.

**Table 2.** Virtual piston based Vuilleumier model and current Vuilleumier models.

	Current	VIRTUAL Piston
pressure		Completely Same
Temperature		Completely Same
Absorbed heat		Completely same
		$W_h = \int PA_h dx_h$ $W_c = \int PA_c dx_c$
work	$W_E = W_h - W_w - W_{r,h}$ $W_C = W_w - W_c + W_{r,c}$ $W_E = Q_h - Q_{w,h} - W_{r,h}$ $W_C = Q_{w,c} - Q_c + W_{r,c}$	$dW_E = PdV_E$

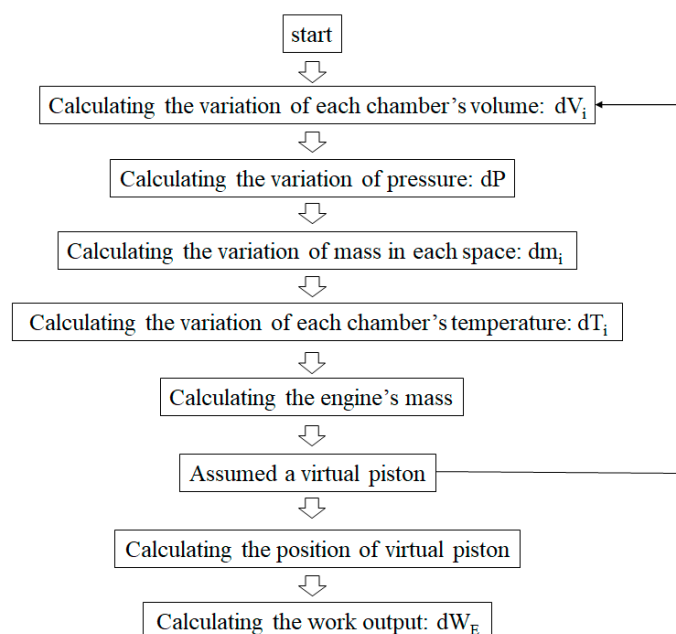


**Figure 6.** Flowchart of simulation process for virtual piston based Vuilleumier model.

### 3. Results and Discussions

In this work, helium was selected as the working fluid. The conditions were set at 550 °C hot temperature, 50~70 °C warm temperature, and −20~10 °C cold temperature.

#### 3.1. Overall Performance of Vuilleumier Machine

Vuilleumier's cooling capacity and COP in the current three chambers Vuilleumier model (TCVM), current four chambers Vuilleumier model (FCVM), and the proposed virtual piston based Vuilleumier model (VPBVM) model were obtained and compared. Figure 7 shows the ratios of  $COP_V$  and  $Q_c$  in FCVM and VPBVM over TCVM at various conditions. The solid line represents FCVM while the dashed line represents VPBVM.

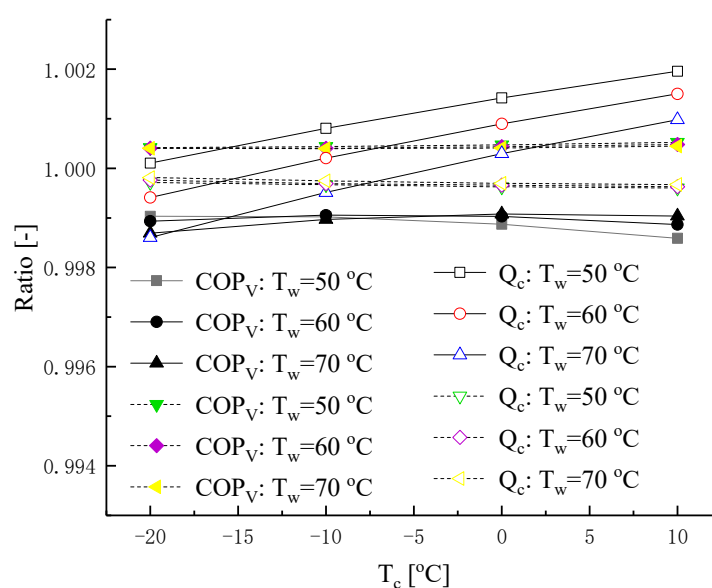


**Figure 7.** Ratios of  $COP_V$  and  $Q_c$  in FCVM and VPBVM over TCVM at various conditions.

As shown in Figure 7, the performances in the three models were the same. This indicates that the overall performance of HVCHP will not be affected by two separate

warm chambers or the virtual piston. In fact, VPBVM only provides a method for tracking the variations of the engine's total volume. The pressure and temperatures in the engine's and cooler's working fluids are coupled as those in TCVM or FCVM. Thus, the overall performance in VPBVM should be the same as those in TCVM and FCVM.

### 3.2. Respective Performance of Hypothetical Engine and Cooler

#### 3.2.1. Respective Performance Based on PV Power Flow in Current Vuilleumier Models

As described above, the engine's output work and cooler's input work for TCVM and FCVM based on PV power flow in this work are determined by

$$W_E = W_h - W_w - W_{r,h} \quad (45)$$

$$W_C = W_w - W_c + W_{r,c} \quad (46)$$

According to Equations (10)–(13), the engine's output work and cooler's input work in TCVM and FCVM can be expressed as

$$W_E = \int PA_h dx_h - \int PA_{w,h} dx_h - \int PA_{r,h} dx_h \quad (47)$$

$$W_C = \int PA_c dx_c - \int PA_{w,c} dx_c + \int PA_{r,c} dx_c \quad (48)$$

As  $A_h = A_{w,h} + A_{r,h}$  and  $A_c = A_{w,c} + A_{r,c}$ , both the engine's output work and cooler's input work in TCVM and FCVM based on Equations (23)–(26) will be zero. This indicates that the determination of PV power flow based on Equations (10)–(13) and Equations (23) and (24) is ineffective for the engine's output work and cooler's input work. This is due to the determinations of engine's and cooler's compression volumes. In independent Stirling machines,  $W_w$  in Equations (45) and (46) is the compression work. However, in Equations (47) and (48), the engine's and cooler's compression volumes are simplified to be the respective swept volume by the respective displacer. In fact, the independent Stirling machine's compression volumes consist of two parts: swept volume by displacer and swept volume by piston. However, the swept volume by piston cannot be obtained in current Vuilleumier models due to there being no piston in Vuilleumier. Thus, this could be the reason for the scarcity of studies on the performance analysis of Vuilleumier's engine and cooler. Moreover, this is the motivation for proposing a virtual piston in the Vuilleumier model.

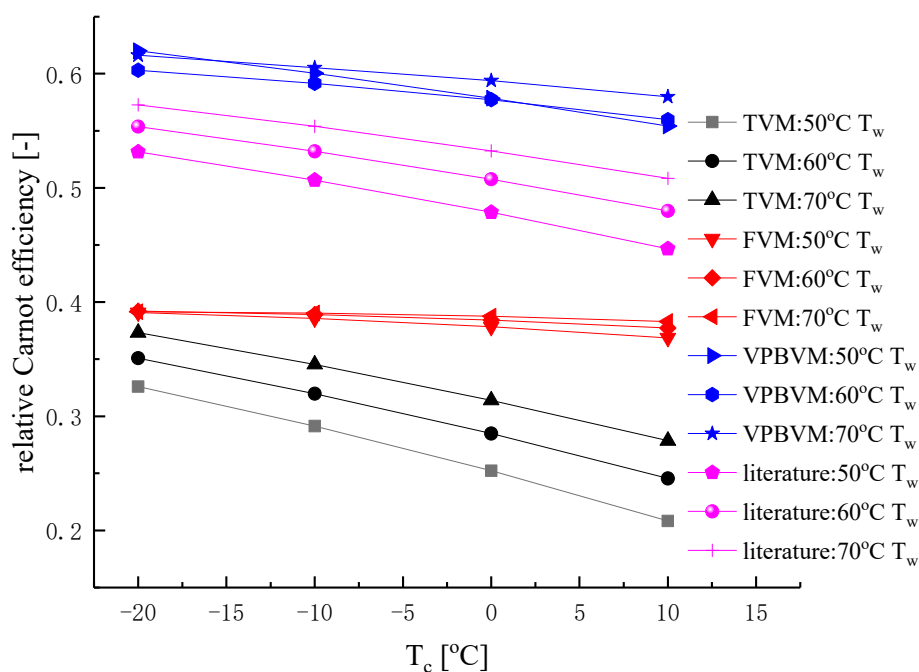
#### 3.2.2. Respective Performance Based on Heat Flow in Current Vuilleumier Models and PV Power Flow in VPBVM

Respective performances of the engine and cooler in TCVM and FCVM are obtained based on heat flow in heat exchangers. Respective performances in VPBVM are obtained based on PV power flow (Equation (28)). Moreover, the results in our previous work [12] are also provided. Figure 8 shows the relative Carnot efficiencies of the engine and cooler at various conditions. Overall, respective values in different models are significantly different, although Vuilleumier's overall performances are the same (as shown in Figure 7).

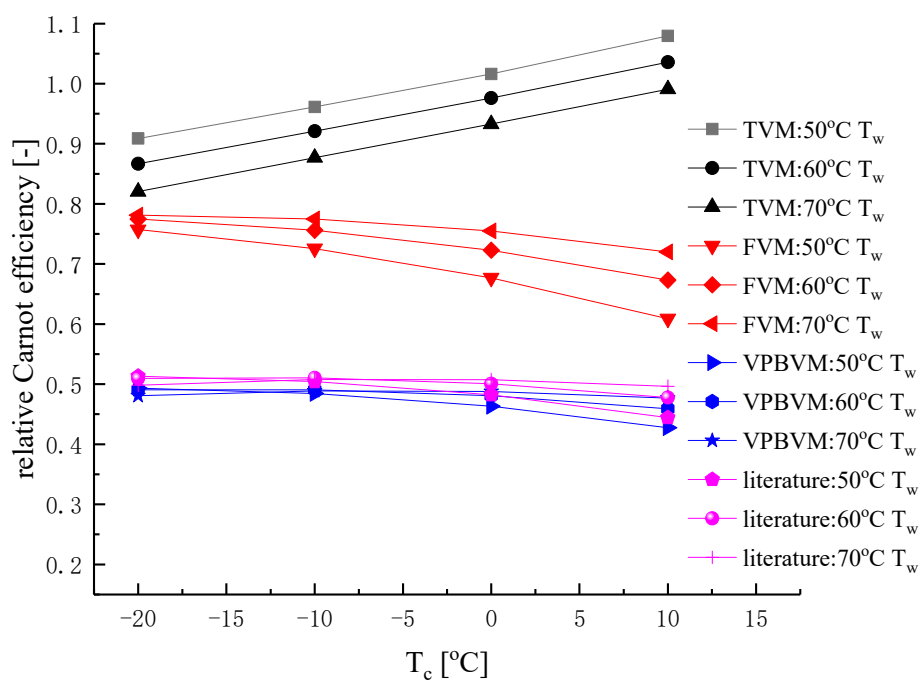
#### Analysis of TCVM

As shown in Figure 8, the engine's relative Carnot efficiency is in the range of 20–37% while the cooler's relative Carnot efficiency is in the range of 82–108% in TCVM. As the cooler's relative Carnot efficiency could not be higher than 100%, it indicates that the engine's output work or cooler's input work is underestimated. This is caused by the shift of heat flow in Vuilleumier's warm chamber. A part of the heat from the cooler's working fluid is transferred to the engine's working fluid. Thus, the dissipated heat in the engine's warm heat exchanger is more than the engine's waste heat. As a result, this leads to lower engine output work based on Equation (23) and lower cooler input work based on

Equation (24). Therefore, it can be concluded that respective performances of the engine and cooler cannot be obtained based on heat flow in TCVM.



(a)



(b)

**Figure 8.** Relative Carnot efficiencies in three models at various conditions: (a) thermal efficiency; (b)  $COP_C$ .

### Analysis of FCVM

As shown in Figure 8, the engine's relative Carnot efficiency is in the range of 37–39% while the cooler's relative Carnot efficiency is in the range of 61–78% in FCVM. Compared to those in TCVM, the engine's relative Carnot efficiency is higher while the cooler's relative Carnot efficiency is lower. As Vuilleumier's overall performance in TCVM and FCVM are the same, the comparisons indicate that two warm chambers with independent temperature can reduce the coupling of heat transfer between the working fluids.

Figure 9 shows the warm temperatures in TCVM's and FCVM's warm chambers during a cycle at conditions of 550 °C  $T_h$ , 70 °C  $T_w$ , and 10 °C  $T_c$ . It can be found that the temperatures of the engine's and cooler's warm chambers in FCVM are not the same. This indicates that heat transfer will occur between the engine's and cooler's working fluids in TCVM. Moreover, the engine's heat dissipated in the engine's warm heat exchanger during 0–90° while the cooler's heat dissipated in the cooler's warm heat exchanger during 90–180°. Thus, the engine's warm temperature during 0–90° and cooler's warm temperature during 90–180° will determine the heat flow. Figure 9 shows that the engine's warm temperature in FCVM is slightly lower than those in TCVM during 0–90° while the cooler's warm temperature in FCVM is slightly higher than those in TCVM during 90–180°. Thus, less heat will be dissipated in the engine's warm heat exchanger while more heat will be dissipated in the cooler's warm heat exchanger. Consequently, this leads to larger engine output work or cooler input work. However, although heat flows in FCVM's two warm heat exchangers are redistributed, the results are still unreasonable since the cooler's relative Carnot efficiencies are too high compared to the results in present studies [5,12]. Therefore, it can be also concluded that respective performances of the engine and cooler cannot be obtained based on heat flow in FCVM.

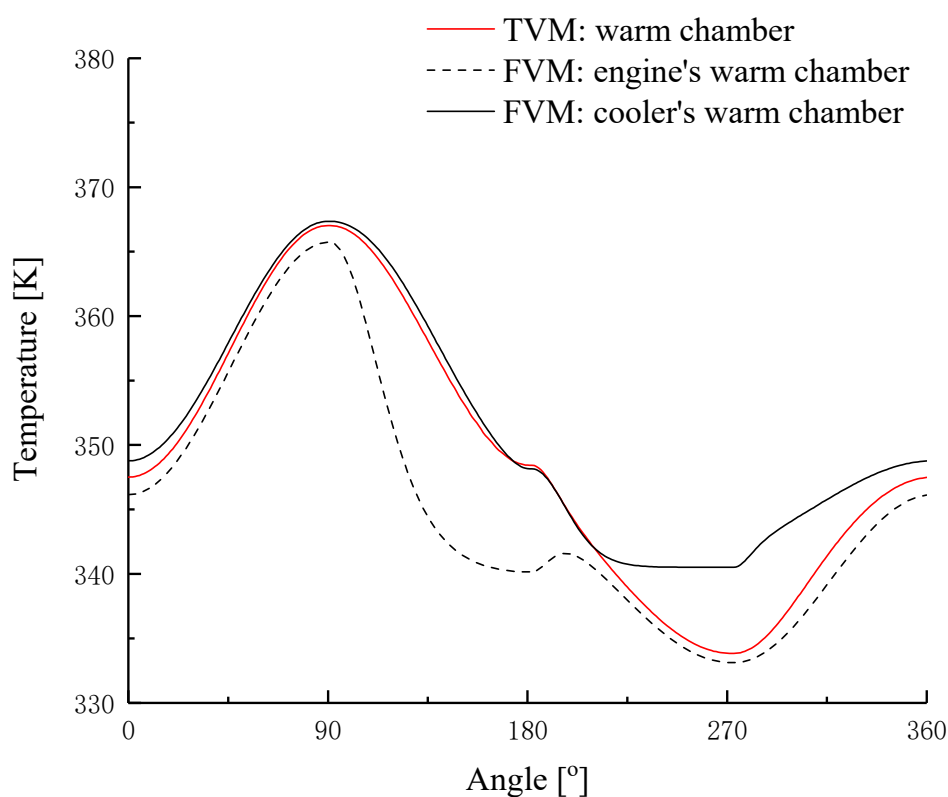


**Figure 9.** Variations of warm chamber's temperature in TCVM and FCVM.

### Analysis of VPBVM

As shown in Figure 8, the engine's relative Carnot efficiency is in the range of 53–64% while the cooler's relative Carnot efficiency is in the range of 43–49% in VPBVM.

As it was difficult to obtain the respective performances in Vuilleumier by experiment, the respective performances obtained by experiments in independent Stirling machines and by the theoretical model in our previous work were used to evaluate the respective performances in VPBVM.

Experimental results showed that thermal-to-mechanical efficiency of the independent Stirling engine was 68% [5] of Carnot efficiency at conditions of 875 °C hot temperature and 80 °C warm temperature, respectively. Compared to the achieved values in the independent Stirling engine, the engine's values in VPBVM do not exceed the maximum value and could be reasonable. Experimental results [6] showed that mechanical-to-thermal efficiency of the independent Stirling cooler was 41–46% of Carnot efficiency at conditions of 45 °C warm head and −30~10 °C cold head. Compared to the achieved values in independent Stirling cooler, cooler's values in VPBVM are slightly higher. This could be due to there being no temperature difference between the heat exchanger temperature and working fluid as a result of the ideal heat exchanger in the theoretical model. Thus, the cooler's values in VPBVM are also reasonable.

Compared to the theoretical results in our previous work [12], the engine's relative Carnot efficiency is 11~18% higher while the cooler's relative Carnot efficiency is 4% lower in VPBVM. Overall, the obtained respective performances in different models are close. As Vuilleumier's overall COP is 6–11% higher than the product of the obtained engine's thermal efficiency and cooler's COP<sub>c</sub> in previous work, this indicates that the engine's thermal efficiency should be underestimated in hybrid mode. If the engine's relative Carnot efficiency is increased by 6–11% in the hybrid model, the gap between the hybrid model and VPBVM will be closer. Therefore, it can be concluded that VPBVM is effective for the analysis of respective performances of the engine and cooler.

Moreover, from Figure 8, it can be found that the engine's relative Carnot efficiency increases with decreasing cold temperature. This could be due to the small compression ratio at higher cold temperature. The variations of the cooler's relative Carnot efficiency are small. Overall, the cooler's relative Carnot efficiency also decreases with increasing cold temperature. This could be caused by higher adiabatic loss at high cold temperature.

### 3.3. Engine's Compression Ratio

At present, the engine's compression ratio in Vuilleumier is usually unclear. However, as the virtual piston can be tracked during a cycle, the variations of the engine's total volume during a cycle were obtained. Thus, engine's compression ratio in Vuilleumier can be obtained in VPBVM. This is defined as

$$\varepsilon = \frac{V_{E,\max}}{V_{E,\min}} \quad (49)$$

Figure 10 shows the compression ratio of engine at various conditions. The compression ratio of the engine is in the range of 1.2–1.24. It decreased with the decreasing temperature ratio of the cooler due to the smaller density variations in the cooler as a result of the low temperature ratio. This could also explain the phenomenon whereby the engine's relative Carnot efficiency increases with decreasing cold temperature (as shown in Figure 8). Egas [25] summarized the experimental compression ratio in the independent Stirling engine. The value was 1.6–1.7 in five machines and 1.39 in one machine. Thus, the compression ratios in the hypothetical engine at such conditions are much lower than the value achieved in the independent Stirling engine. This could lead to lower thermal efficiency in a Stirling engine with losses [3] since the effect of losses would be larger at low compression ratio.

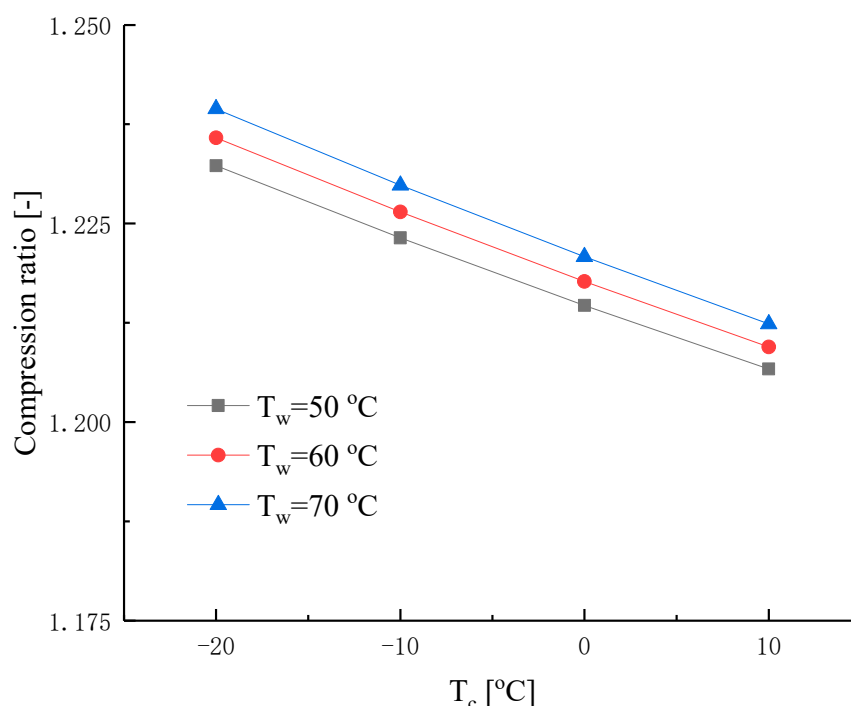


Figure 10. Compression ratio of Vuilleumier's engine at various conditions.

#### 4. Conclusions

This study investigated the respective performances of a hypothetical Stirling engine and cooler in a Vuilleumier machine based on PV power flow and heat flow methods. A virtual piston based Vuilleumier model was developed. The following conclusions were made:

- (1) The overall performances of the Vuilleumier machine were the same in VPBVM and the current adiabatic model. Thus, the assumption of a virtual piston will not affect the evaluation of Vuilleumier performance. In fact, VPBVM only provides a method for tracking the variations of the engine's total volume. The pressure and temperatures in the engine's and cooler's working fluids are the same as those in current Vuilleumier models.
- (2) Both PV power flow and heat flow methods were employed for the analysis of the hypothetical Stirling engine's and Stirling cooler's performance in current Vuilleumier models. The results showed that these methods were ineffective in the analysis of the hypothetical Stirling engine and Stirling cooler in Vuilleumier machines. It also indicates that respective performances of the hypothetical Stirling engine and Stirling cooler cannot be obtained based on experiments, since experiments are usually based on PV power flow and heat flow methods.
- (3) The assumption of a virtual piston in VPBVM provides a solution to track the variations of the engine's and cooler's compression volumes. Thus, variations of the engine's and cooler's volumes during the cycle can be monitored. As a result, the respective performances of the Vuilleumier's engine and cooler can be obtained based on VPBVM. Moreover, the engine's compression ratio can be obtained in VPBVM. The obtained engine's compression ratio explained that a relatively smaller thermal efficiency was obtained at high cold temperature in Vuilleumier machines. Moreover, the obtained engine's compression ratio could be used in the optimization of the Vuilleumier's engine and cooler. However, the VPBVM in this work is based on the assumption of an engine's total working fluid. Variations of the engine's total working fluid could lead to small variations in respective performance.

Opportunities for further work include the analysis, preliminary design, and optimization of Vuilleumier machines and the analysis of conventional Vuilleumier machines with sinusoidal motions based on VPBVM.

**Author Contributions:** Conceptualization, B.L.; Investigation, Q.L. and Q.G.; Resources, J.L. and Y.H.; Software, J.Y.; Supervision, B.L.; Writing—original draft, Q.L.; Writing—review & editing, J.L., Y.H. and C.R. All authors have read and agreed to the published version of the manuscript.

**Funding:** This research received no external funding.

**Institutional Review Board Statement:** Not applicable.

**Informed Consent Statement:** Not applicable.

**Data Availability Statement:** Data can be available with the approval of all the authors.

**Conflicts of Interest:** The authors declare no conflict of interest.

## Nomenclature

### Variable

$A$	Area ( $\text{m}^2$ )
$C_v$	specific heat at constant volume ( $\text{J}\cdot\text{kg}^{-1}\cdot\text{K}^{-1}$ )
$C_p$	specific heat at constant pressure ( $\text{J}\cdot\text{kg}^{-1}\cdot\text{K}^{-1}$ )
$COP$	coefficient of performance
$m$	working fluid's mass (kg)
$Q$	heat (J)
$P$	pressure (kPa)
$R$	gas constant ( $\text{kJ}\cdot\text{kg}^{-1}\cdot\text{K}^{-1}$ )
$T$	temperature (K)
$T_i^*$	working fluid's temperature to the interface between chamber and heat exchanger (K)
$V$	volume ( $\text{m}^3$ )
$W$	work (J)
$x$	displacer's displacement (m)
$\eta$	thermal efficiency (-)
$\varepsilon$	compression ratio
$\gamma$	ratio of specific heat
$\varphi$	angle ( $^\circ$ )
Subscript	
1,2, ... ,9	shown in Figure 3
2E	volume occupied by engine in warm chamber, which is marked in green in Figure 5a
2i, 2o, 4i, 4o	shown in Figure 4
7E	volume occupied by engine in cold-warm heat exchanger, which is marked in green in Figure 5c
8E	volume occupied by engine in cold regenerator
ce, wr, rc, wc, rh, he	interface shown in Figure 4
c	cold
C	cooler
Carnot	relative Carnot efficiency
con	conduction loss
E	engine
h	hot
r	rod
R	regenerator loss
shuttle	shuttle loss
practical	practical machine
V	Vuilleumier machine
w	warm

## References

1. Carlsen, H. Results from 20 kW Vuilleumier heat pump test program. In Proceedings of the Intersociety Energy Conversion Engineering Conference, Monterey, CA, USA, 7–12 August 1994.
2. Woods, J.; Bonnema, E. Regression-based approach to modeling emerging HVAC technologies in EnergyPlus: A case study using a Vuilleumier-cycle heat pump. *Energy Build.* **2019**, *186*, 195–207. [\[CrossRef\]](#)
3. Guo, T.; Jiang, T.; Zou, P.; Luo, B.; Hofbauer, P.; Liu, J.; Huang, Y. Analytical model for Vuilleumier cycle. *Int. J. Refrig.* **2020**, *113*, 126–135. [\[CrossRef\]](#)
4. Bakker, E.J.; Garde, J.V.D.; Jansen, K.; Wagener, P. *Gas Heat Pumps: Efficient Heating and Cooling with Natural Gas*; Gas Terra/Castel International: Groningen, The Netherlands, 2010.
5. Free Piston Stirling Engine Based 1 kW Generator. Available online: [https://arpa-e.energy.gov/sites/default/files/6\\_Sunpower.pdf](https://arpa-e.energy.gov/sites/default/files/6_Sunpower.pdf) (accessed on 15 September 2021).
6. Janssen, M.; Beks, P. Measurement and Application of Performance Characteristics of a Free Piston Stirling Cooler. 2002. R3-3. Available online: <https://citeseerx.ist.psu.edu/viewdoc/download?doi=10.1.1.682.4376&rep=rep1&type=pdf> (accessed on 13 September 2021).
7. Dogkas, G.; Rogdakis, E. A review on Vuilleumier machines. *Therm. Sci. Eng. Prog.* **2018**, *8*, 340–354. [\[CrossRef\]](#)
8. Kühl, H.-D.; Shulz, S. Measured Performance of an Experimental Vuilleumier Heat Pump in Comparison To 3rd Order Theory. In Proceedings of the 25th Intersociety Energy Conversion Engineering Conference, Reno, NV, USA, 12–17 August 1990.
9. Kawajiri, K.; Honda, T.; Sugimoto, T. Study of Free Piston Vuilleumier Heat Pump. Basic Performance Analysis. *JSME Int. J. Ser. B* **1997**, *40*, 617–625. [\[CrossRef\]](#)
10. Pfeffer, T.; Kühl, H.-D.; Schulz, S.; Walther, C. Entwicklung und Experimentelle Untersuchung Neuer Regeneratorkonzepte für Regenerative Gaskreisprozesse am Beispiel Einer Vuilleumier-Wärmepumpe. *Forsch Ingenieurwes* **2000**, *65*, 257–272. [\[CrossRef\]](#)
11. Kuehl, H.-D.; Schulz, S.; Walther, C. Thermodynamic Design and Optimization of a 20 kW Vuilleumier Heat Pump. *SAE Technical Paper Series* **1999**. [\[CrossRef\]](#)
12. Zou, P.; Gao, Q.; Wang, S.; Yang, J.; Luo, B.; Hofbauer, P.; Liu, J.; Huang, Y.; Ren, C. A method of analyzing the respective performances of hypothetical stirling engine and stirling cooler in Vuilleumier machine. *Int. J. Refrig.* **2020**, *118*, 376–383. [\[CrossRef\]](#)
13. Chen, H.; Longtin, J.P. Performance analysis of a free-piston Vuilleumier heat pump with dwellbased motion. *Appl. Therm. Eng.* **2018**, *140*, 553–563. [\[CrossRef\]](#)
14. Sowale, A.; Kolios, A.J.; Fidalgo, B.; Somorin, T.; Parker, A.; Williams, L.; Collins, M.; McAdam, E.; Tyrrel, S. Thermodynamic analysis of a gamma type Stirling engine in an energy recovery system. *Energy Convers. Manag.* **2018**, *165*, 528–540. [\[CrossRef\]](#)
15. Cheng, C.H.; Yang, H.S.; Keong, L. Theoretical and experimental study of a 300-W beta-type Stirling engine. *Energy* **2013**, *59*, 590–599. [\[CrossRef\]](#)
16. Udeh, G.T.; Michailos, S.; Ingham, D.; Hughes, K.J.; Ma, L.; Pourkashanian, M. A new non-ideal second order thermal model with additional loss effects for simulating beta Stirling engines. *Energy Convers. Manag.* **2020**, *206*, 112493. [\[CrossRef\]](#)
17. Li, R.; Grosu, L. Parameter effect analysis for a Stirling cryocooler. *Int. J. Refrig.* **2017**, *80*, 92–105. [\[CrossRef\]](#)
18. Alireza, B.; Ali, K. A Gamma type Stirling refrigerator optimization: An Experimental and Analytical investigation. *Int. J. Refrig.* **2018**, *91*, 89–100.
19. Luo, B.J.; Zou, P.; Jiang, T.; Gao, Q.; Liu, J. Decoupled duplex Stirling machine: Conceptual design and theoretical analysis. *Energy Convers. Manag.* **2020**, *210*, 112704. [\[CrossRef\]](#)
20. Georges, H.A.; Christophe, A.; Malahi, A.; François, L. Thermodynamic Analysis of the Stirling Duplex Machine. *Adv. Eng. Forum.* **2018**, *30*, 80–91.
21. Liao, C.; Jiang, T.; Hofbauer, P.; Ye, W.; Liu, J.; Luo, B.; Huang, Y. Simplified model and analysis for the performance of Hofbauer–Vuilleumier heat pump. *Int. J. Refrig.* **2019**, *103*, 126–134. [\[CrossRef\]](#)
22. Homutescu, V.M.; Bălănescu, D.T.; Popescu, A. Adiabatic Behavior of the Vuilleumier Heat Pump. *IOP Conf.* **2018**, *444*, 082025. [\[CrossRef\]](#)
23. Suganami, T.; Kawajiri, K.; Honda, T. Vuilleumier Cycle Heat Pump. In Proceeding of the 1989 JAR Annual Conference. 1990. Available online: <https://www.sciencedirect.com/science/article/pii/B9780080401935500687> (accessed on 13 September 2021).
24. Kawajiri, K.; Honda, T.; Sugimoto, T. Study of free piston Vuilleumier heat pump: Performance characteristics of prototype machine during forced vibration. *Trans. Jpn. Soc. Mech. Eng. B* **1997**, *40*, 626–634. [\[CrossRef\]](#)
25. Egas, J.; Clucas, D.M. Stirling engine configuration selection. *Energies* **2018**, *11*, 584. [\[CrossRef\]](#)